RRB-87-61

# MONTE CARLO DETERMINATIONS OF VOLUME REFLECTANCE FOR NATURAL WATERS

by

J.H. Jerome, R.P. Bukata
and J.E. Bruton

Rivers Research Branch
National Water Research Institute
Canada Centre for Inland Waters
Burlington, Ontario, Canada L7R 4A6
NWRI Contribution #87-149

## MANAGEMENT PERSPECTIVE

Monte Carlo computer techniques are a valuable means of theoretically modelling the propagation of incident radiation through natural water masses. Consequently, the Rivers Research Branch at NWRI has developed such a Monte Carlo program and applied it to various aspects of radiative transfer processes occurring in inland waters.

This communication compares the NWRI model with similar models used by the University of Miami and CSIRO, Australia in predicting the subsurface volume reflectance (ratio of upwelling to downwelling irradiance at a particular depth). The Miami model is primarily directed towards oceanic waters, while the CSIRO model is primarily directed towards inland waters. The NWRI model accommodates both types of natural waters by illustrating the necessity to segment the Monte Carlo curve fitting into two sets of relationships, one appropriate to ocean waters and one appropriate to inland waters. The oceanic results (lower range of volume reflectance values) agree favourably with the Miami results, while the inland waters results (higher range of volume reflectance values) more accurately represent inland waters than does the CSIRO model, due, probably, to the added attention given to the volume scattering distribution function by NWRI, particularly for small-angle forward scattering.

The NWRI model also carefully considers a variety of incident irradiance distributions.

PERSPECTIVE - GESTION

Les techniques informatiques de Monte Carlo constituent un bon moyen de modéliser théoriquement la propagation du rayonnement incident dans les masses d'eau naturelles. Par conséquent, la Direction de la recherche sur les rivières de l'INRE a mis au point un programme Monte Carlo et l'a appliqué à divers aspects des processes de transfert radiatif propres aux eaux intérieures.

Le présent exposé compare le modèle de l'INRE avec des modèles semblables utilisés par l'Université de Miami et le CSIRO en Australie pour prévoir la réflectance volumétrique sous la surface de l'eau (rapport entre l'éclairement énergétique de la montée de l'eau et celui de la descente de l'eau à une profondeur donnée). Le modèle de Miami porte principalement sur les eaux océaniques et celui du CSIRO, principalement sur les eaux intérieures. Le modèle de l'INRE se prête aux deux types d'eau naturelle en établissant qu'il faut segmenter l'ajustement des courbes du modèle Monte Carlo en deux ensembles d'équations, l'un propre aux eaux océaniques et l'autre, aux eaux intérieures. Les résultats océaniques (gamme inférieure des valeurs de réflectance volumétrique) correspondent assez bien avec les résultats de Miami, tandis que les résultats des eaux intérieures (gamme supérieure des valeurs de réflectante volumétrique) représentent de façon plus précise les eaux intérieures que le modèle du CSIRO, probablement à cause de la plus grande attention portée par l'INRE à la fonction distribution de diffusion volumétrique, particulièrement en ce qui a trait à la diffusion vers l'avant aux petites valeurs angulaires.

Le modèle de l'INRE prend également en considération une variété de distributions d'éclairement énergétique incident.

## ABSTRACT

A Monte Carlo simulation of photon propagation through natural waters was utilized to develop the relationships among subsurface volume reflectance R, incident irradiance distribution (defined by above-water zenith angle $\theta'$ and in-water angle of refraction $\theta_0$), and the inherent optical properties scattering to absorption ratio b/a and backscattering probability B. A natural demarcation at Bb/a=0.25 was observed which conveniently serves to suggest appropriate relationships for primarily inland (i.e. higher values of Bb/a) and for primarily oceanic (i.e. lower values of Bb/a) waters. For the ranges $0 \leq Bb/a \leq 0.25$ and $0.25 \leq Bb/a \leq 0.50$, respectively, the relationships are

$$R(\theta') = \frac{0.319}{\mu_0} \frac{Bb}{a}$$

and

$$R(\theta') = \frac{1}{\mu_0} \left[0.267 \frac{Bb}{a} + 0.013\right]$$

where $\mu_0 = \cos \theta_0$. For a cardioidal incident distribution $\mu_0$ may be taken to be 0.858.

RÉSUMÉ

Une simulation de Monte Carlo de la propagation des photons dans les eaux naturelles a été utilisée pour élaborer les équations de la réflectance volumétrique R sous la surface, de la distribution d'éclairement énergétique incident (défini par l'angle θ' entre le zénith au-dessus de l'eau et l'angle de réfraction $\theta_0$ dans l'eau), des propriétés optiques inhérentes du rapport diffusion/absorption b/a et de la probabilité de rétrodiffusion B. On a observé une démarcation naturelle au point Bb/a=0,25 qui permet de suggérer des équations appropriées surtout pour les eaux intérieures (c.-à-d. les valeurs supérieures de Bb/a) et surtout pour les eaux océaniques (c.-à-d. les valeurs inférieures de Bb/a). En ce qui a trait au plages $0 \leq Bb/a \leq 0,25$ et $0,25 \leq Bb/a \leq 0,50$, les équations sont respectivement :

$$R(\theta') = \frac{0.319}{\mu_0} \frac{Bb}{a}$$

et

$$R(\theta') = \frac{1}{\mu_0} \left[0.267 \frac{Bb}{a} + 0.013\right]$$

où $\mu_0 = \cos \theta_0$. Dans le cas d'une distribution cardioïdale incidente, $\mu_0$ serait égal à 0,858.

Monte Carlo simulations of photon propagation through natural waters have recently become a valuable technique in modelling the interactions among the downwelling incident radiation fields and the inherent optical properties of the water. The subsurface volume reflectance (ratio of upwelling to downwelling irradiance at a particular depth) is a direct consequence of such interactions among the incident radiation field and the inherent optical properties.

The classic work of Gordon et al[1] utilized such Monte Carlo simulations to arrive at expressions for subsurface volume reflectance, as well as expressions for other apparent optical properties. Two volume reflectance expressions were reported therein, one applicable to collimated incidence ($0° \leq \theta_0 \lesssim 20°$) and one applicable to both diffusive incidence as well as collimated incidence ($\theta_0 \gtrsim 30°$), where $\theta_0$ is the in-water angle of refraction for the collimated incident radiation. No single equation for the angular response of volume reflectance R with $\theta_0$ was given in Gordon et al[1].

Using a Monte Carlo simulation, Kirk[2,3] has also derived relationships among volume reflectance, incident radiation distribution, and aquatic optical properties. In these works, however, volume reflectance expressions were obtained for vertical incidence, and as a function of $\theta'$, the angle of incidence of the collimated incident radiation.

Monte Carlo simulations of photon propagation through natural waters have been used at the National Water Research Institute, and it is the intention of this Letter to compare the outputs of our simulations with those of Gordon et al[1] and Kirk[2,3].

In our simulations, the selected values of b/a (ratio of the scattering coefficient to the absorption coefficient of the water) were 1, 3, 5, 8, 10, 12, and 18. A volume scattering phase function with a backscattering probability B=0.0253 was taken from Petzold[4]. For such a volume scattering phase function, values of the volume scattering distribution function were determined for scattering angles of 0.1°, 0.2°, 0.4°, 0.8°, 1.0°, and at 1° intervals up to 180°. Particular attention was ascribed to scattering angles <1° to accommodate the dominating impact of scattering phenomena at small angles. The incident radiation distributions considered included collimated fields defined by $\theta'$=0°, 30°, 45°, 60°, and 89° ($\theta'$ is the angle of incidence of the impinging radiation measured from the vertical) as well as a diffusive cardioidal distribution.

Figure 1 illustrates our Monte Carlo relationship between $R(\theta')$ and Bb/a for the case of vertical incidence (i.e. $\theta'$=0°). In order to accommodate the Monte Carlo outputs (shown as points in Figure 1) with a linear relationship, it is necessary to segment the range of Bb/a values. A demarcation value of Bb/a=0.25 is readily suggested. The two linear relationships depicted in Figure 1 are:

$$R(0^\circ) = 0.319 \frac{Bb}{a} \tag{1}$$

for $0 \leq Bb/a \leq 0.25$

and $$R(0^\circ) = 0.267 \frac{Bb}{a} + 0.013 \tag{2}$$

for $0.25 \leq Bb/a \leq 0.50$.

The range of volume reflectances ($0 \leq R \leq 0.15$) considered in Figure 1 encompasses that which would be observed for most naturally occurring ocean and/or inland waters.

Figure 2 illustrates the response of volume reflectance $R(\theta')$ to varying the angle of incidence $\theta'$. Herein are plotted the values of the ratio $R(\theta')/R(0°)$ as a function of $1/\mu_0$ where $\mu_0$ is the cosine of the in-water refracted angle $\theta_0$ for the incident radiation distribution characterized by $\theta'$. These values of $R(\theta')/R(0°)$ are taken as the arithmetic mean of this ratio for the seven values of Bb/a considered in this work. The standard deviations of these $R(\theta')/R(0°)$ ratios are indicated by the vertical bars in Figure 2. The larger standard deviations for $1/\mu_0=1.315$ and 1.512 (i.e. $\theta'=60°$ and 89°, respectively) are a consequence of an apparent second-order relationship between $R(\theta')$ and $R(0°)$ which increases with $\theta'$. The linear relationship of Figure 2 is defined by:

$$R(\theta') = \frac{R(0°)}{\mu_0} \tag{3}$$

where $\mu_0 = \cos \theta_0$.

In a similar manner, our Monte Carlo simulation, considering a diffusive cardioidal distribution as the incident radiation field, yields the relationship:

$$R = 1.165\ R(0°) \tag{4}$$

where R indicates the subsurface volume reflectance associated with a diffusive cardioidial, rather than a collimated incident radiation field.

Comparing equations (3) and (4) suggests the value of $\mu_0$ to be 0.858, in excellent agreement with the value of 0.859 calculated by Prieur and Sathyendranath[8] as being appropriate for cardioidal incidence.

Table I lists the predicted values of volume reflectance resulting from equations (1) to (4) considering collimated incident distributions defined by $\theta'=0°$, 30°, 45°, 60°, and 89°, as well as a diffusive cardioidal incident distribution. For each incident distribution, the values of volume reflectance for Bb/a = 0.02, 0.08, 0.24, and 0.48 are tabulated. For comparison, the corresponding volume reflectance values of Gordon et al[1] and Kirk[2,3] are also given.

The saline features of Table I include:

a) Significant differences between our and the Gordon et al[1] predictions are clearly in evidence for collimated incident fields with large zenith angles $\theta'$. This is a consequence of the Gordon et al[1] volume reflectance relationships being appropriate for either a diffuse incident distribution or for collimated incident distributions characterized by small zenith angles. Their use of a single relationship for diffuse incidence as well as for collimated incidence at larger values of $\theta'$ is not particularly appropriate for $\theta'$ values $\geq 60°$.

b) Significant differences between our and the Gordon et al[1] predictions occur for intermediate to high values of Bb/a (i.e as the volume reflectance increases so also, generally, does the disparity between the two predictions). However, as the Gordon et al[1] work was directed predominantly towards oceanic applications, it is understandable that preferential curve fitting was given to lower values of Bb/a. As seen from their Figure 7[1], their single equation underestimates their Monte Carlo outputs for the larger volume reflectances. Our predominant concern with inland water applications necessitated our segmentation of the range of Bb/a values into two regimes, with a separate volume reflectance equation required for each segment. For the $0 \leq Bb/a \leq 0.25$ range, which quite adequately covers the range normally encountered in oceans, there is very little disparity between our results and the results of Gordon et al[1]. For the $0.25 \leq Bb/a \leq 0.50$ range, the use of an independently curve-fitted equation to the Monte Carlo outputs enables, we feel, the meaningful predictions of volume reflectance for inland waters.

c) Significant differences between our and the Kirk[2,3] predictions occur for large incident angles and high Bb/a values. This could be due, in part, to his[2,3] partitioning of the volume scattering phase function into 5° intervals to obtain the volume scattering distribution function, while our partitioning was into 1° intervals with the first 1° segmented into five parts.

## REFERENCES

1. H.R. Gordon, O.B. Brown, and M.M. Jacobs, Appl. Opt. 14, 417 (1975).
2. J.T.O. Kirk, Aust. J. Mar. Freshwater Res. 32, 517 (1981).
3. J.T.O. Kirk, Limnol. Oceanogr. 29, 350 (1984).
4. T.J. Petzold, Volume Scattering Functions for Selected Waters (Scripps Institution of Oceanography, University of California at San Diego, 1972), SIO Ref. 72-78.
5. L. Prieur and S. Sathyendranath, Limnol. Oceanogr. 26, 671 (1981).

TABLE I: Comparison of Monte Carlo Determinations of Volume Reflectance

| Incident Distribution | $\frac{Bb}{a}$ | Volume Reflectance | | |
|---|---|---|---|---|
| | | Gordon et al[1] | Kirk[2,3] | Present Work |
| Direct, 0° | .02 | .0065 | .0066 | .0064 |
| | .08 | .025 | .026 | .026 |
| | .24 | .069 | .079 | .077 |
| | .48 | .125 | .157 | .141 |
| Direct, 30° | .02 | .0065 | .0078 | .0069 |
| | .08 | .025 | .031 | .028 |
| | .24 | .069 | .094 | .083 |
| | .48 | .125 | .188 | .152 |
| Direct, 45° | .02 | .0076 | .0088 | .0075 |
| | .08 | .029 | .035 | .030 |
| | .24 | .079 | .106 | .090 |
| | .48 | .141 | .212 | .167 |
| Direct, 60° | .02 | .0076 | .0099 | .0084 |
| | .08 | .029 | .040 | .034 |
| | .24 | .079 | .119 | .101 |
| | .48 | .141 | .238 | .186 |
| Direct, 89° | .02 | .0076 | .0111 | .0096 |
| | .08 | .029 | .045 | .039 |
| | .24 | .079 | .134 | .116 |
| | .48 | .141 | .268 | .213 |
| Cardioidal | .02 | .0076 | .0085 | .0074 |
| | .08 | .029 | .034 | .030 |
| | .24 | .079 | .102 | .089 |
| | .48 | .141 | .205 | .164 |

## FIGURE CAPTIONS

Figure 1: Relationship between $R(\theta')$ and Bb/a for the case of vertical incidence (i.e. $\theta'=0°$).

Figure 2: Relationship between the ratio $R(\theta')/R(0°)$ and the inverse of the cosine of the in-water angle of refraction ($1/\mu_0$).

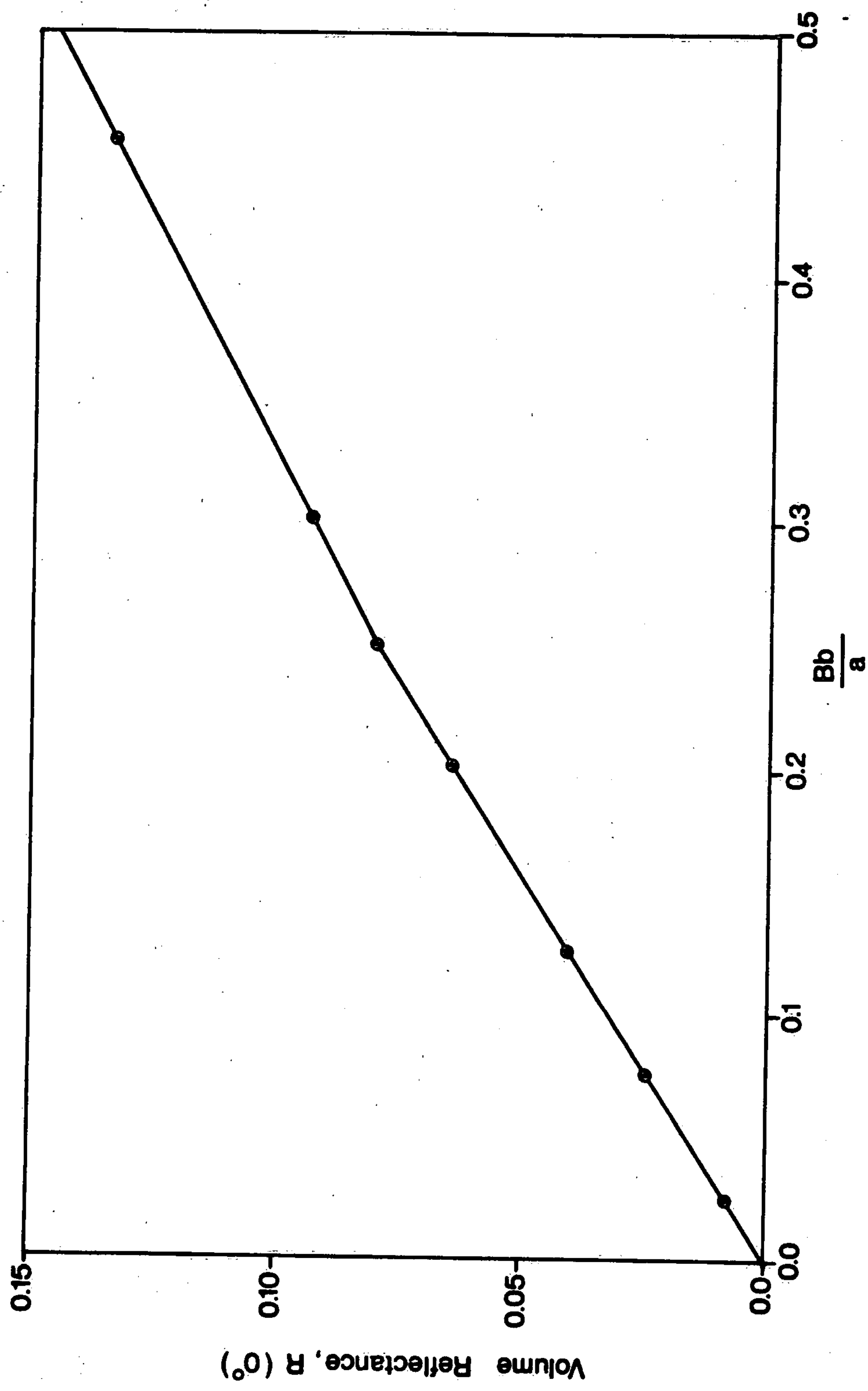


FIGURE 1

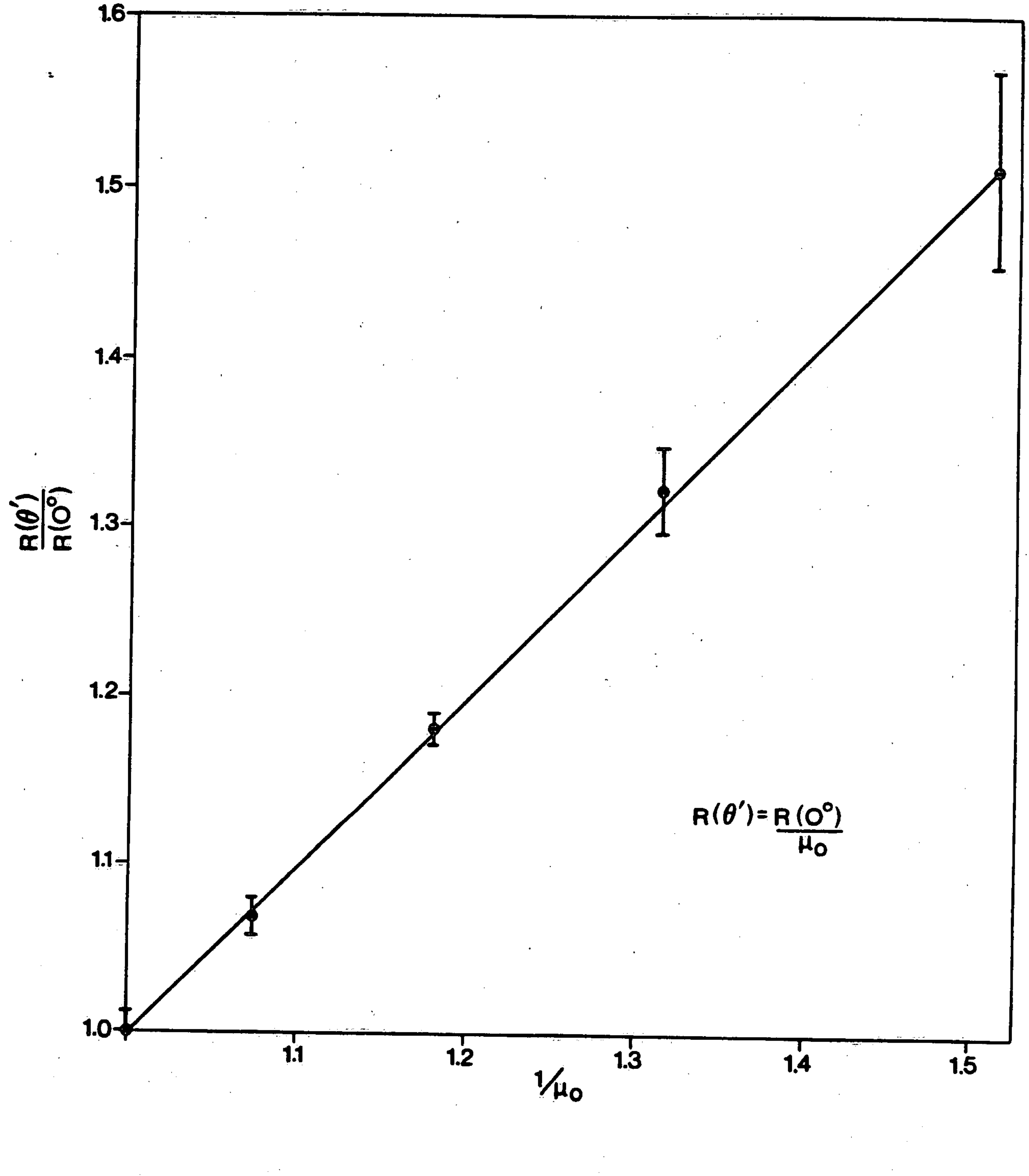
1.6
1.5
1.4
1.3
1.2
1.1
1.0
$\frac{R(\theta')}{R(0^\circ)}$
$R(\theta') = \frac{R(0^\circ)}{\mu_0}$
1.1
1.2
1.3
1.4
1.5
$1/\mu_0$

FIGURE 2